the strong coupling between them overshadows the changing properties of the substrate introduced by the misalignment of the material and waveguide axes.

IV. CONCLUSION

This article demonstrates the use of the MoM for the analysis of the scattering characteristics of various microstrip discontinuities in transmission lines within a shielded structure. It represents the first comprehensive study that highlights the effects of substrate anisotropy on the frequency response of three MIC discontinuities commonly encountered in practice. The analytical formulation and its numerical implementation for all structures are validated against existing data. Ample new numerical results that demonstrate the effects of rotating the axes of the material tensors on the S parameters are also included. It is observed that, in general, the influence of the material anisotropy becomes more prominent as the frequency increases. However, it is also shown that substrate anisotropy is not always the dominant factor that governs the dispersion characteristics of the MIC discontinuity. Other factors, such as proximity effects due to the presence of the side walls close to the discontinuity (e.g., stub) can overshadow the influence of changing material properties of the substrate.

ACKNOWLEDGMENT

This work was supported by the U.S. Army Research Office under Grant No. DAAL03-92-G-0275.

REFERENCES

1. N. G. Alexopoulos, "Integrated-Circuit Structures on Anisotropic Substrates," *IEEE Trans. Microwave Theory Tech.*, Vol. MTT-33, No. 10, Oct. 1985, pp. 847–881.
2. Special issue on Gyroelectric Waveguides and their Circuit Applications, *IEE Proc. Pt. H*, Vol. 140, no. 3, June 1993.
3. M. Geshiro, S. Yagi, and S. Sawa, "Analysis of Slotlines and Microstrip Lines on Anisotropic Substrates," *IEEE Trans. Microwave Theory Tech.*, Vol. MTT-39, No. 1, Jan. 1991, pp. 64–69.
4. Y. Chen and B. Beker, "Dispersion Characteristics of Open and Shielded Microstrip Lines under a Combined Principal Axes Rotation of Electrically and Magnetically Anisotropic Substrates," *IEEE Trans. Microwave Theory Tech.*, Vol. MTT-41, No. 4, April 1993, pp. 673–679.
5. J. Martel, R. R. Boix, and M. Horno, "Static Analysis of Microstrip Discontinuities Using the Excess Charge Density in the Spectral Domain," *IEEE Trans. Microwave Theory Tech.*, Vol. MTT-39, No. 9, Sept. 1991, pp. 1623–1631.
6. J. Martel, R. R. Boix, and M. Horno, "Design Parameters of Asymmetric Edge-Coupled Microstrip Open-Ended Discontinuities," *Microwave Opt. Technol. Lett.*, Vol. 5, No. 9, Aug. 1992, pp. 411–417.
7. S. S. Toncich, R. E. Collin, and K. B. Bhasin, "Full-Wave Characterization of Microstrip Open End Discontinuities Patterned on Anisotropic Substrates Using Potential Theory," *IEEE Trans. Microwave Theory Tech.*, Vol. MTT-41, No. 12, Dec. 1993, pp. 2067–2073.
8. H-Y. Yang and N. G. Alexopoulos, "Characterization of Finline Step Discontinuity on Anisotropic Substrates," *IEEE Trans. Microwave Theory Tech.*, Vol. MTT-35, No. 11, Nov. 1987, pp. 956–963.
9. Y. Chen and B. Beker, "Study of Microstrip Step Discontinuities on Bianisotropic Substrates Using the Method of Lines and Transverse Resonance Technique," *IEEE Trans. Microwave Theory Tech.*, Vol. 42, No. 10, Oct. 1994, pp. 1945–1950.
10. J. Cain and B. Beker, "Analysis of Microstrip Step Discontinuities in MICs Printed on Anisotropic Substrates Using the Method of Moments," *Microwave Opt. Technol. Lett.*, Vol. 7, No. 12, Aug. 1994, pp. 574–577.
11. R. W. Jackson, "Full-Wave, Finite Element Analysis of Irregular Microstrip Discontinuities," *IEEE Trans. Microwave Theory Tech.*, Vol. MTT-37, No. 1, Jan. 1989, pp. 81–89.
12. L. Wu and H. Chang, "Analysis of Dispersion and Series Gap Discontinuity in Shielded Suspended Striplines with Substrate Mounting Grooves," *IEEE Trans. Microwave Theory Tech.*, Vol. MTT-40, No. 2, Feb. 1992, pp. 279–284.

Received 12-15-94

Microwave and Optical Technology Letters, 9/2, 77–83

CCC 0895-2477/95

TRAVELING-WAVE SEMICONDUCTOR LASER AMPLIFIER INDUCED INTERMODULATION DISTORTION FOR DIFFERENT DIGITAL MODULATION SCHEMES IN A SUBCARRIER MULTIPLEXING SYSTEM

Yang-Han Lee
Department of Electrical Engineering
Tamkang University
Tamsui, Taipei Hsien, Taiwan 25137

Chao-Nan Tsai, San-Liang Lee, and Jingshown Wu
Department of Electrical Engineering
National Taiwan University, Republic of China

KEY TERMS

Semiconductor lasers, laser amplifiers, intermodulation, multiplexing

ABSTRACT

We analyze the intermodulation distortion (IMD) induced by four-wave mixing in traveling-wave semiconductor laser amplifiers (TWSLA) for different digital modulation schemes in a subcarrier multiplexing (SCM) system, and compare these results with the transmission of pure tones. We find that the IMDs are reduced in the digital modulation system, because the modulated signals disturb the homogeneous property of amplitude (ASK, FSK) or phase (PSK). We conclude that PSK has better performance, and the worst case is the transmission of pure tones.

INTRODUCTION

Traveling-wave semiconductor laser amplifiers (TWSLA) are very attractive in communication systems. In a subcarrier multiplexing (SCM) system, the intermodulation distortion (IMD) induced by four-wave mixing (FWM) will need to be taken into account. This phenomenon has been of interest for several authors [1–3]. According to those results, if signals with uniform amplitude and phase, that is, pure tones, are transmitted, the IMDs will become dominant when the system has a large number of channels and close channel space. In this article, we will show that the IMDs will be reduced while using a digital modulation scheme (such as ASK, FSK, or PSK), and make a comparison between them.

ANALYSIS

In the active layer of TWSLA, the total optical fields can be expressed in the form

$$E = \frac{1}{2} \sum_{j=-(M-2)}^{2M-1} E_j(z,t) \exp[i(\omega_j t - k_j z)] + \text{c.c.} \quad (1)$$

The carrier density N can be obtained by solving the rate equation

$$\frac{\partial N}{\partial t} = \frac{J}{ed} - \frac{N}{\tau_s} - \frac{a(N-N_0)}{\hbar\omega}|E|^2. \quad (2)$$

We assume the optical field with equal spacing and N in the form [4]

$$N = N_e + \Delta N \quad (3)$$

and

$$\Delta N = \sum_{m=1}^{3M-3} (\Delta N_m e^{im\Omega t} + \text{c.c.}) + \Delta N_0, \qquad N_e = \frac{J\tau_s}{qd}, \quad (4)$$

where J is the injected current density, τ_s is the carrier lifetime, q is the electron charge, d is the active layer thickness, a is the differential gain, N_0 is the carrier density for the transparency, Ω denotes channel spacing, M denotes input channel numbers, and c.c. denotes the complex conjugate.

The normalized optical field E and ΔN_m are given as

$$\tilde{E} = \frac{E}{E_s}, \qquad \Delta n_m = \frac{\Delta N_m}{N_0 - N_e}. \quad (5)$$

After some mathematic derivation, we get the general solution

$$\sum_{m=-(3M-3)}^{3M-3} D'_{m-l}\,\Delta n_l = D_m, \quad (6)$$

$$D'_{m-l} = \begin{cases} D_{m-l}, & \text{if } l \neq m, \\ 1 + im\Omega\tau_s + D_0, & \text{if } l = m, \end{cases}$$

$$D_m = \sum_{j=-(M-2)+m}^{2M-1} \tilde{E}_j \tilde{E}_{j-m}, \quad (7)$$

where E_s denotes the saturated field amplitude, and D_m denotes the products of the fields separated m times the channel spacing. It is usually reasonable to neglect the mutual coupling among Δn_m and the fields. Therefore we get

$$\Delta n_0 = \frac{D_0}{1 + D_0}, \quad (8)$$

$$\Delta n_m = \frac{D_m}{(1 + im\Omega\tau_s + D_0)(1 + D_0)}. \quad (9)$$

The total electric field $\tilde{E}$ along the amplifier is governed by the wave equation and use of the polarization P:

$$P = \epsilon_0 \chi(N) E = i\epsilon_0 \frac{nc}{\omega}(1 + i\alpha) g_m(N) E. \quad (10)$$

This results in

$$\frac{\partial \tilde{E}_j}{\partial z_j} = \frac{\Gamma g_0(1 + i\alpha) - \alpha_{\text{int}}}{2} \tilde{E}_j - \frac{\Gamma g_0(1 + i\alpha)}{2} \sum_{l=-(M-2)}^{2M-1} \Delta n_{j-l} \tilde{E}_l,$$
$$j = -(M-2) \cdots 2M - 1, \quad (11)$$

where g_0 denotes the unsaturated gain coefficient, α_{int} is the model absorption coefficient, Γ is the optical mode confinement factor, and α is the linewidth enhancement factor.

From the above expression, the specified field in the TWSLA is influenced by other fields. While solving the coupling equation, we devide the cavity into K pieces uniformly ($K = 300$ in the following examples). For each interval, Δz_j, we record the terms induced by other fields as a noise. To interpret the concept, we rewrite the equation as follows:

$$\frac{\Delta \tilde{E}_j}{\Delta z_j} = \left[\frac{\Gamma g_0}{2}(1 + i\alpha - \alpha_{\text{int}} - \Delta n_0 - i\alpha\,\Delta n_0)\right] \tilde{E}_j - \left[\frac{\Gamma g_0(1 + i\alpha)}{2} \sum_{l=-(M-2), l\neq j}^{2M-1} \Delta n_{j-l} \tilde{E}_l\right]. \quad (12)$$

We regard the second bracket of the right-hand side as a noise inside the specified field $\tilde{E}_j$ in the interval Δz_j, and sum those of $\Delta \tilde{E}_j$ as the overall noise inside $\tilde{E}_j$.

We consider the four different cases in the SCM system. The probability of 0 and 1 is equal in each channel of the following system.

1. For pure tones transmitted, the N channel waves enter the amplifier simultaneously with the same power and uniform phase; the IMDs will be the largest.
2. For the ASK system, the extinction ratio is defined as the ratio of high power and low power; low power will be transmitted for signal 0 and high power for signal 1. This will improve the performance of Case 1 by 3 dB, because the amplitudes are no longer homogeneous.
3. For the FSK system, the signals 0 and 1 will locate at different frequencies f_1 and f_2. In order to make a comparison with the others, we let the value $f_2 - f_1$ be equal to a half bandwidth per channel, and consider $N/2$ channels only; that is, we regard the two channels of the ASK system as one channel here. We find that this improves the performance of Case 1 by about 10 dB, for the same reason as above.
4. We consider the PSK system. We shall distinguish two signals 0 and 1 from different phases, 0° phase for signal 0 and 180° phase shift for signal 1. The IMDs in this case are much lower than the others, because this will seriously disturb the coherent property of the phase. To interpret this, consider that two input channels with 180° phase shift, from the view of the time domain, when the amplitude of one channel is positive, the other is negative. It is predictable that the interaction between them is small; therefore, IMDs are reduced rapidly. The results are shown in Figure 1.

One of the important parameters in SCM system is the carrier-to-noise ratio (CNR). Here we consider the CNR with only the noise induced from FWM in TWSLA. In general the CNR must be above 17 dB. We defined the input sensitivity as the input power to achieve the minimum CNR $\approx$ 20 dB of all the channels in the SCM system. We consider, for small channel spacing, that input sensitivities will be reduced when the channel numbers increase, because increasing the channel numbers will lead to increased power scattering out of the amplified input signal band. The relationships between channel numbers versus input sensitivities and corresponding output powers inside the band of amplified input signals are shown in Figure 2.

CONCLUSION

The IMDs in the TWSLA induced by FWM have been studied here. We find they are reduced for different digital modulation schemes in SCM system, because the modulated signals disturb the homogeneous property of amplitude (ASK, FSK) or phase (PSK). We conclude that the capacity of anti-IMD effects are PSK > FSK > ASK, and the worst case is the transmission of pure tones.

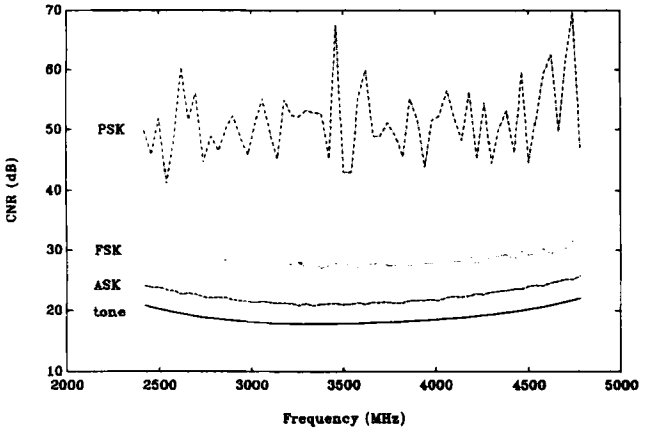

Figure 1 The amplified input frequency band and corresponding CNR of a SCM system with 60-channel input and equal channel spacing, 40 MHz, in the range between 2.4 and 4.8 GHz, where CNR is defined as the ratio of the average output powers of amplified input signals and the level of IMD effects inside a single channel. $P_{in} = -30$ dBm, $P_{out} \approx -11$ dBm, $P_s = 12.4$ dBm. In an ASK system, the extinction ratio is equal to 20, $L = 300$ μm, $\Gamma = 0.225$, $\alpha_{int} = 24$ cm^{-1}, $g_0 = 760$ cm^{-1}, $\alpha = 6$, $\tau_s = 0.22$ ns

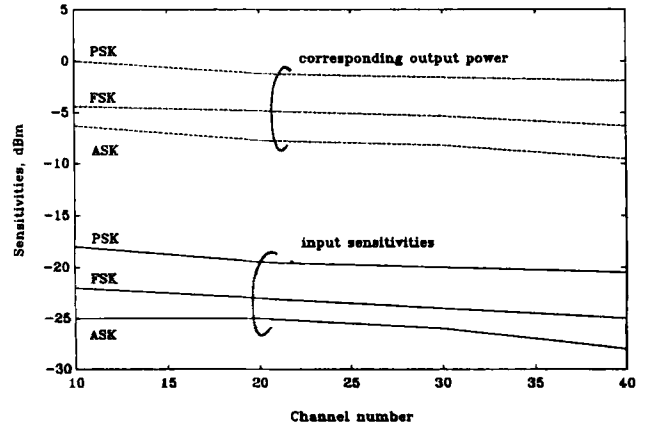

Figure 2 Channel numbers versus input sensitivities (solid lines) and corresponding output power inside the band of amplified input signals (dashed lines). The parameters are the same as in Figure 1

REFERENCES

1. Y. C. Chung, J. M. Wiesenfeld, G. Raybon, U. Koren, and Y. Twu, "Intermodulation Distortion in a Multiple-Quantum-Well Semiconductor Optical Amplifier," *Photon. Technol. Lett.*, Vol. 3, No. 2, 1991, pp. 130–132.
2. R. M. Jopson and T. E. Darcie, "Calculation of Multicarrier Intermodulation Distortion in Semiconductor Optical Amplifiers," *Electron. Lett.*, Vol. 24, No. 22, 1988, pp. 1372–1374.
3. T. E. Darcie, R. M. Jopson, R. W. Tkach, "Intermodulation Distortion in Optical Amplifiers from Carrier-Density Modulation," *Electron. Lett.*, Vol. 23, No. 25, 1987, pp. 1392–1394.
4. Takaaki Mukai and Tadashi Saitoh, "Detuning Characteristics and Conversion Efficiency of Nearly Degenerate Four-Wave Mixing in a 1.5 μm Traveling-Wave Semiconductor Laser Amplifier," *J. Quantum Electron.*, Vol. 26, No. 5, 1990, pp. 865–975.

Received 11-30-94

Microwave and Optical Technology Letters, 9/2, 83–85

CCC 0895-2477/95

ANALYSIS OF SOME COPLANAR TRANSMISSION LINES: COPLANAR COUPLED LINES, COPLANAR COUPLED STRIPLINES, AND COPLANAR COUPLED LINES WITH RECTANGULAR MICROSHIELD

Naichang Yuan, Jianguo He, Demiao Yao, Qin Dai, and Weigan Lin
Department of Electronic Technology
National University of Defence Technology of China
Changsha 410073, People's Republic of China

KEY TERMS

Coplanar waveguide, coplanar coupled lines, microshield

ABSTRACT

Two types of coplanar transmission lines, rectangular microshield coplanar coupled lines (RMCCL) and coplanar coupled rectangular microshield lines (CCRML), are proposed for MMIC applications. These are developed from coplanar coupled lines (CCL) and coplanar coupled strip lines (CCS). Analytic formulas are presented for calculating the quasistatic TEM parameters of these coupled lines by means of exact conformal mapping techniques. Numerical results are also presented to illustrate the properties of these coplanar transmission lines. © 1995 John Wiley & Sons, Inc.

I. INTRODUCTION

Coplanar waveguides (CPW) [1], because they can be easily adapted to external shunt element connection as well as for monolithic integrated circuits (MIC) fabrication on semiinsulating substrates, have received much attention in the fields of microwave and millimeter wave integrated circuits (MMIC). Coplanar coupled lines (CCL), like coupled microstrip lines or strip lines, may find application in directional couplers [2]. Furthermore, it is balanced transmission lines that are useful for balanced circuits such as mixers and differential drivers such as those in some high-speed digital applications [3].